

ELECTRON BEAM BUNCH PROFILE DETERMINATION THROUGH CERENKOV RADIATION

X. K. Maruyama*, J. R. Neighbours, F. R. Buskirk
 Department of Physics
 Naval Postgraduate School
 Monterey, California 93943

*Visiting from National Bureau of Standards, Gaithersburg, MD 20899

Abstract

The spatial charge distribution of an electron pulse, along with the beam interaction length, determines the Cerenkov radiation distribution as a function of frequency. An angular distribution of the Cerenkov radiation can, in principle, measure its spatial charge distribution. At a measurement angle of 90° with respect to the beam direction, the form factor is unity which allows a measurement of the total charge contained in the pulse. At other angles, Fourier transforms of the charge distribution may be measured. Possible application to intense relativistic beams in air is discussed.

Introduction

Because the distribution of intensity of Cerenkov radiation is proportional to the frequency, the radiation at sub-optical frequencies is low for a single charged particle. It has been shown, however, that microwave Cerenkov radiation is observable when the electron beam is intense and bunched so that coherent radiation by many charged particles contribute. Previous works by the NPS group^{1,2} calculated in detail and observed the radiation intensity at microwave frequencies for bunches periodic in time. Most of the findings may be applied directly to Cerenkov radiation from a single bunch. Among them are the observation that a) If each bunch has a spatial distribution described by a charge density $\rho(r)$, the radiated intensity is modified by the Fourier transform of this charge distribution; b) At frequencies such that the wavelength of the emitted radiation is of the order of the bunch size, the electrons of the bunch radiate coherently, leading to large enhancements of the radiated power. Destructive interference described by the Fourier transform of the charge distribution decreases the intensity with increasing frequency, until incoherent radiation takes over when the wavelength of the radiation is less than the electron spacing; c) If the region in which the beam interacts with the medium is of finite length, the radiation propagation direction is not confined to a sharp Cerenkov angle, but is spread over a range of emission angles. The usual description of the Cerenkov radiation being emitted as a Mach front is a special case of a diffraction pattern where the interaction length is infinitely long compared to the radiation wavelength.

In this paper we will illustrate examples of the consequence of the finite spatial charge distribution to show that Cerenkov radiation emitted at low frequencies may be used to characterize the properties of an intense relativistic beam in air.

Radiation From a Single Charge Bunch

The result of Ref. 1 may be rewritten so that the radiated energy per solid angle per unit frequency by an electron bunch propagating a distance L can be written as a particularly simple expression

$$E(\nu, k) = QR^2 d\nu \quad 1$$

where Q is a constant defined by

$$Q = \frac{\mu c q^2}{8\pi} \quad 2$$

The quantity q is the total charge in the electron bunch, c is the speed of light in the medium and μ is the magnetic permeability of the medium. The radiation function R is

$$R = kL \sin \theta I(u) F(k) \quad 3$$

and the parameters are

$$u = \frac{kL}{2} (\cos \theta_0 - \cos \theta) \quad 4$$

$$I(u) = \sin u / u. \quad 5$$

The ordinary Cerenkov angle is given by $\cos \theta_0 = 1/n\beta$ where n is the index of refraction of the medium and k is the wave vector in the medium. F(k) is a dimensionless form factor, i.e. the Fourier transform of the charge bunch is $qF(k)$. Where the spatial charge distribution of the electron bunch is a line charge in the lab frame at $t = 0$, $\rho(r) = \rho(z)\delta(x)\delta(y)$, then, $qF(k) = qF(k_z) = \int dz \exp(-ik_z z)\rho(z)$ and $k_z = k \cos \theta$. The observation angle θ is the angle between the radiation and the beam axis. I(u) is a diffraction function arising from the finite value of kL. In the limit that $kL \rightarrow \infty$, the diffraction function behaves like δ function such that the Cerenkov radiation is observed when $u = 0$, i.e. $\theta = \theta_0$. This is the familiar classical limit for optical Cerenkov radiation.

The form factor is identically one for a point charge, and for a finite distribution $F(k) = 1$ for $k = 0$. F(k) must fall off as a function of k near the origin if all the charge has the same sign. Analogous to the form factor in electron scattering used to determine the nuclear charge distribution, for small values of k_z , the form factor for Cerenkov radiation characterizes the extent of a line charge pulse. Higher frequencies would provide information concerning higher moments of the charge distribution.

Illustrative Cases

We consider a trapezoidal beam pulse illustrated in Fig. 1. The form factor for the trapezoid is given by the expression

$$F(k_z) = \frac{4}{k^2(d^2-b^2)} (\sin^2(k_z d/2) - \sin^2(k_z b/2)) \quad 6$$

Two cases of this distribution are presented here.

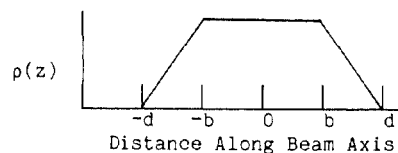


Fig. 1. Charge Distribution of beam pulse. For case I, b = 5 m and d = 10 m. Case II is a pulse of half the length with b = 2.5 m and d = 5 m.

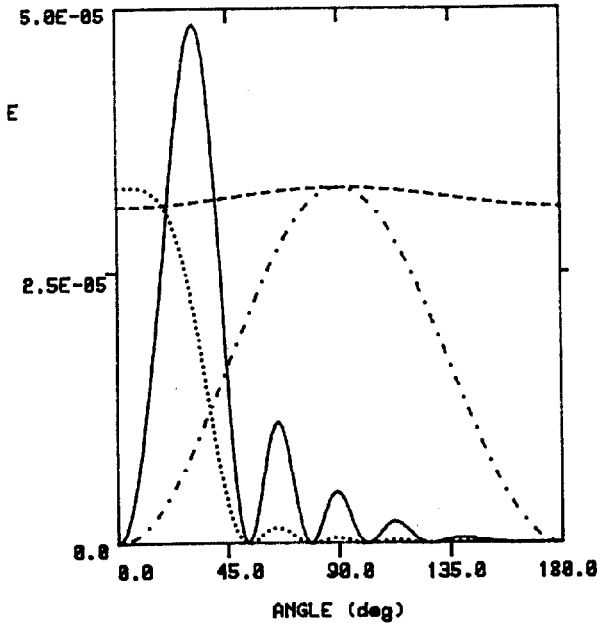


Fig. 2. Functions contributing to Eq. 1. The solid line is the total radiated energy in a unit frequency interval per solid angle per bunch (joules/sr/Hz). The dashed line is the square of the form factor and the dotted line is the diffraction function $I^2(u)$. The dot-dash curve is $\sin^2\theta$. F^2 , I^2 and $\sin^2\theta$ all have maximum values of unity. The electron beam energy is 50 MeV. The charge distribution of case I with a peak current of 10 kA is assumed. The interaction length $L = 300$ m in air. The Cerenkov radiation frequency is 2.5 MHz corresponding to a wavelength of 120 m.

Fig. 2 presents the functions which contribute to Eq. 1. As the frequency is increased, the form factor begins to probe the details of the bunch structure. Fig. 3 illustrates this effect where the wavelength is about the same as the beam bunch length. The enhancement of the radiated energy at 90° arises because $k_z = 0$ and the form factor is unity there. When the radiation wavelength is small compared to the beam dimensions, the enhancement of the form factor at 90° dominates the radiation pattern. Fig. 4 shows the case for a radiated frequency of 100 MHz.

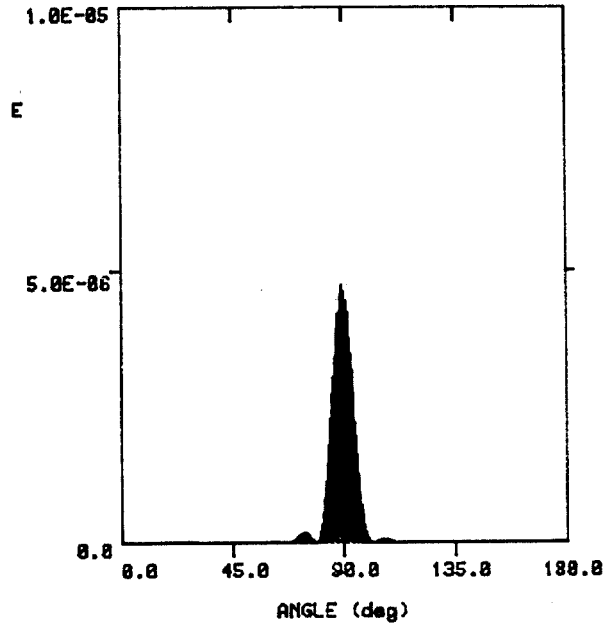


Fig. 4. The energy per solid angle for radiation at 100 MHz corresponding to a wavelength of 3 m. The parameters of Fig. 2 are assumed for a case I charge distribution.

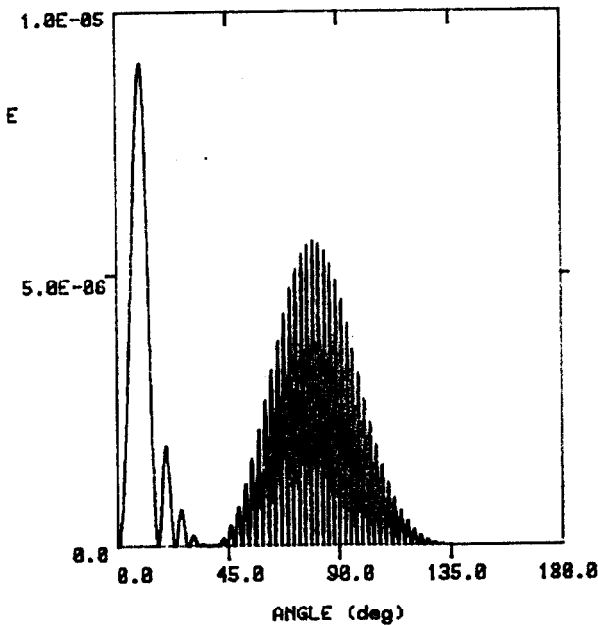


Fig. 3. The energy per solid angle for radiation at 25 MHz corresponding to a wavelength of 12 m. The parameters of Fig. 2 are assumed for a case I charge distribution.

Fig. 5 plots the form factors for the beam pulse as a function of θ . As frequency is increased, the form factor exhibits more structure corresponding to the higher moments of the charge distribution.

If the beam pulse is varied, the frequency dependence of the radiation pattern changes. For case II, a beam pulse of half the length of case I is assumed. In Fig. 6 two examples of case II beam pulse are presented for 2.5 MHz. At low frequency the radiated energy is proportional to the square of the total charge contained in the pulse. In Fig. 7 it is shown that for 25 MHz the enhancement of the radiated energy at $\theta = 90^\circ$ is not as striking as for the case I pulse in Fig. 3 as the wavelength is still larger than the beam pulse length. For 100 MHz, the enhancement at 90° for the shorter pulse is similar to that for the longer pulse. Fig. 5 also presents the form factors for the two different pulse shapes considered in this paper. For 2.5 MHz the form factors are nearly unity and not significantly different for the two cases, whereas for 25 MHz the form factors are measurably different.

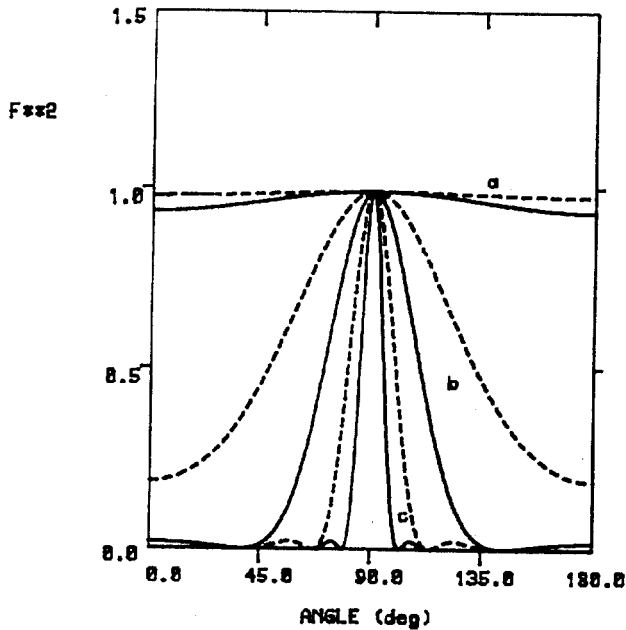


Fig. 5. Squares of the form factor as a function of the radiation angle. Each solid line represents case I and each dotted line represents case II beam pulse shapes. a, b and c are for frequencies of 2.5, 25 and 100 MHz, respectively.

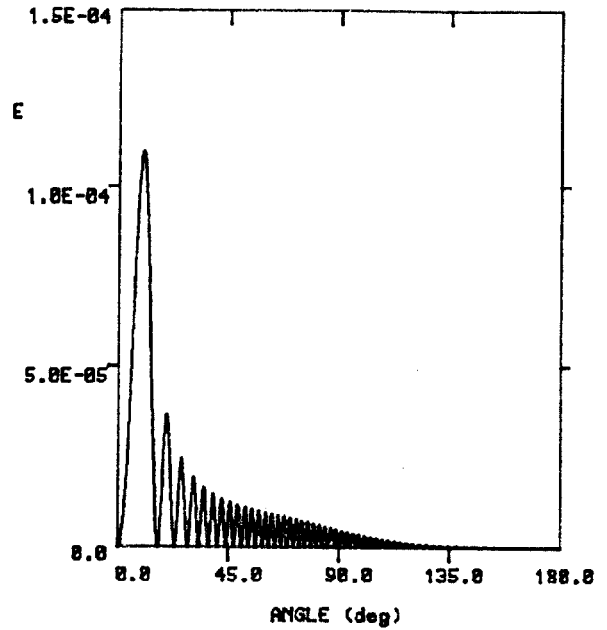


Fig. 7. Radiated energy per solid angle for radiation at 25 MHz for a case II pulse of the same charge but half the length of the corresponding case I pulse. All other parameters are identical to that of Fig. 3.

Discussion

The illustrative examples presented here suggest that sub-optical low frequency Cerenkov radiation might be used as a detection and diagnostic tool to characterize the properties of an intense relativistic beam pulse after it has left the accelerator and entered the air. A complete angular map of the envelope of the radiation pattern could provide a measure of $F(k_z)$ and in analogy to the determination of nuclear charge distributions with electron scattering, the beam pulse charge distribution can be obtained.

The examples presented here are idealized and there has been no attempt to take into consideration such factors as beam pulse erosion as it traverses the atmosphere. Other effects which must be addressed before this approach is experimentally realizable include the ground plane reflection resulting in interference. The considerations presented here does point out that radiation perpendicular to the beam direction should be observed.

The work was partially supported by the Defense Advanced Research Projects Agency.

References

1. F.R. Buskirk and J.R. Neighbours, Phys. Rev. A28, 1531 (1983).
2. J.R. Neighbours, F.R. Buskirk and A. Saglam, Phys. Rev. A29, 3246 (1984).

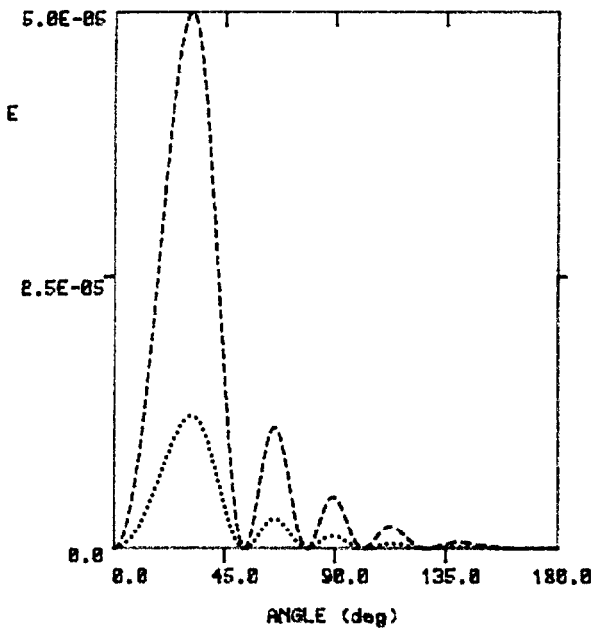


Fig. 6. Radiated energy per solid angle for 2.5 MHz for a case II pulse of half the length as for the previously discussed case. The dashed curve corresponds to the same total charge and the dotted curve corresponds to the same peak current as for the pulse in Fig. 2. All other parameters remain unchanged.